Macromolecules
ARTICLE

Macromolecules **2010**, *43*, 10481–10489

DOI: 10.1021/ma102395p

Molecular Structure and Surface Properties of Comb-Like Fluorinated Poly(oxyethylene)s Having Different Content of Fluoroalkyl Side Group

Jae-Seung Chung,[†] Byoung Gak Kim,[†,‡] Eun-Ho Sohn,[†] and Jong-Chan Lee*,[†]

[†] *Department of Chemical and Biological Engineering, Seoul National University, Shilim-9-Dong, Gwanak-Gu, Seoul 151-744, Korea, and* [‡] *Fuel Cell Center, Korea Institute of Science and Technology, 39-1 Hawolgok-dong, Sungbuk-gu, Seoul, 136-791, Korea*

Received April 27, 2010; Revised Manuscript Received November 16, 2010

ABSTRACT: A series of comb-like fluorinated poly(oxyethylene)s having different content of fluoroalkyl side group were prepared to examine the effect of the surface structure variation on the surface properties. When the thin films of the polymers having ≥ 58 mol % of fluoroalkyl side groups were annealed, surface energy decreased and surface stability against polar liquids improved. This surface property behavior was found to be very well correlated with changes of the paracrystalline structure orientation and scattering unit numbers after the annealing process. However the average tilt angle and *d* spacing of the fluoroalkyl side group and the paracrystalline ordering of the thin films did not change, if any, after the annealing process. Near-edge X-ray absorption fine structure (NEXAFS) spectroscopy and grazing incidence X-ray diffraction (GIXD) were used to determine the surface structure, and contact angle measurements were conducted to measure the surface properties.

1. Introduction

Fluorinated polymers have been studied intensively because of their excellent properties, such as low surface energy, good chemical and thermal stability, antiadhesive ability, low friction coefficient, biocompatibility, and nonstick behavior.[1−3] Researchers have particularly focused on comb-like fluorinated polymers for their excellent surface properties arising from the well-ordered surface molecular structure for use as water/oil repellent and antifouling coating materials.[4−6] In general, the molecular structure of comb-like fluorinated polymer has a key influence on the surface properties, such as the surface energy, stability, adhesion force, repellency, and wetting behavior.[7−12] Takahara et al. reported the molecular aggregation structure and surface properties of the poly(fluoroalkyl acrylate)s and poly(fluoroalkyl methacrylate)s having fluoroalkyl side groups with different fluorocarbon lengths, and the fluorinated polyacrylates having long fluoroalkyl side groups (number of fluorocarbon ≥ 8) were found to have an ordered structure with high water repellency.[13−15] Ober et al. synthesized various fluorinated block copolymers having low surface energy[16] and examined their molecular structure using near-edge X-ray absorption fine structure (NEXAFS)[17−20] and grazing incidence X-ray diffraction (GIXD) measurements.[21] A previous study examined the effects of side chain interconnecting groups of comb-like fluorinated polystyrenes on the bulk and surface properties.[22] Various reports have been published on the comb-like fluorinated polymers, whereas only a few studies have investigated the influence of the content of fluoroalkyl side group on the surface properties of comb-like fluorinated polymers.[23−25]

A paracrystal, which is an intermediate stage between a "perfect crystal" and "amorphous structure", as a "building block", has become accepted as a basic physical concept for defining certain ordered structures. In molecular structure studies of semicrystalline polymers, several models, including the Hosemann paracrystal model, Cialle model, and modified Cialle model have been used to describe ordered polymer structures.[26−28] Recently, the paracrystalline theory proposed by Hosemann[29,30] was considered to be the most suitable model for examining polymer structures having lamellar structures.[13,14,31,32] Indeed, lamellar structures are one of the most common morphological structures observed in polymers, including those in comb-like fluorinated polymers.[13,16,22,31]

Previously, it was reported that comb-like poly(oxyethylene)s containing hydrocarbon alkyl or fluoroalkyl side groups show well-ordered structures due to phase separation between the flexible hydrophilic oxyethylene backbone part and hydrophobic side group part.[24,33−40] Furthermore, comb-like poly(oxyethylene)s containing fluoroalkyl side group have very low surface energies owing to the well-ordered structures near the outmost surface.[24] This study examined the correlation between the surface properties and molecular structures of comb-like fluorinated poly(oxyethylene)s possessing different contents of fluoroalkyl side group. The Hosemann paracrystal model was used to evaluate the paracrystalline structure ordering and orientation in the polymer thin films. The effect of the paracrystalline structure ordering and orientation to the surface properties of comb-like fluorinated polymers having different content of fluoroalkyl side group were systematically studied. NEXAFS and GIXD techniques were used to characterize the molecular structures on the surface, and contact angle measurements were performed to analyze the surface properties, such as surface energy and stability.

2. Experimental Section

2.1. Materials. Epichlorohydrin (Aldrich) was dried over calcium chloride and distilled fractionally from calcium oxide. Methylene chloride and methanol were refluxed over calcium hydride, and 1,1,2-trichlorotrifluoroethane (F113) was refluxed over calcium chloride and freshly distilled under a nitrogen atmosphere prior to use. 1*H*,1*H*,2*H*,2*H*-Perfluorodecanethiol (Aldrich), triphenylcarbenium hexafluorophosphate (Aldrich), sodium (Aldrich), *d*-chloroform (ACROS), and an ionic liquid, 1-butyl-3-methyl-imidazolium chloride ([bmim][Cl]) (C-TRI) were used without further purification.

---

*Corresponding author. Tel: +82 2 880 7070. Fax: +82 2 888 1604. E-mail: jongchan@snu.ac.kr.

© 2010 American Chemical Society

Published on Web 11/30/2010

Table 1. Reaction Conditions, Degree of Substitution, and Thermal Properties of TP-Xs[a]

	sodium perfluorodecane thiolate (mol %)	degree of substitution (mol %)	T_g (°C)	transition, °C (ΔH, mJ/mol)
TP-48	55	48	41.3	90.4 (4.1)
TP-58	65	58	41.8	90.3 (4.2)
TP-72	75	72	46.4	87.8 (14.1)
TP-83	85	83	54.3	86.9 (19.2)
TP-90	100	90		90.2 (26.6)
TP-100	120	100		91.8 (50.1)

[a] Reaction temperature and time were 70 °C and 15 min, respectively.

2.2. Synthesis. *Preparation of Poly[oxy(chloromethyl)ethylene].* Triphenylcarbenium hexafluorophosphate (0.05 g, 0.13 mmol) was added to a stirred solution of epichlorohydrin (5.0 g, 54.04 mmol) in 3.78 mL of methylene chloride under a nitrogen atmosphere. This reaction mixture was stirred at 0 °C for 72 h. The product was purified by precipitating from a tetrahydrofuran (THF) solution in methanol twice and then dried under vacuum at room temperature for 72 h. This product was obtained in 33% yield after the purification steps (fractional precipitation). The weight-average molecular weight (M_w) and polydispersity index of the polymer measured using gel permeation chromatography (GPC) were 5000 and 1.3, respectively. ^{1}H NMR of poly[oxy(chloromethyl)ethylene] ($CDCl_3$, δ): 3.71 (m, 5H).

Preparation of Poly[oxy[[2-(perfluorooctyl)ethyl]thiomethyl]-ethylene]s (TP-Xs, Where X is the mol % of Monomeric Units Containing Fluoroalkyl Side Group). Comb-like fluorinated poly(oxyethylene)s were prepared by a polymer analogous reaction of poly[oxy(chloromethyl)ethylene] with sodium 1*H*,1*H*,2*H*,2*H*-perfluorodecane-1-thiolate, as previously reported.[40] Poly[oxy(chloromethyl)ethylene] (0.076 g, 0.82 mmol) was dissolved in an ionic liquid, 1-butyl-3-methyl-imidazolium chloride ([bmim][Cl]) (10 g), at 70 °C. This was followed by the addition of sodium 1*H*,1*H*,2*H*,2*H*-perfluorodecane-1-thiolate, which had been prepared by a reaction of sodium with 1*H*,1*H*,2*H*,2*H*-perfluorodecanethiol. Table 1 lists the mole percentage of sodium 1*H*,1*H*,2*H*,2*H*-perfluorodecane-1-thiolate used and the degree of substitution. The reaction mixture was stirred at 70 °C for 15 min and then poured in a water/methanol mixture. The precipitate was further purified by several precipitations from F113 into methanol. After further extraction with methanol for 12 h using a Soxhlet extractor, the polymer was dried overnight under a higher vacuum. The product was obtained in $>80\%$ yield. We calculated the degree of substitution using the ^{1}H NMR results by comparing the multiplet at 2.39 ppm (2H) from the fluorinated alkyl side group and the multiplet at 3.64 (3H) from the backbone, which included the contribution of residual poly[oxy(chloromethyl)ethylene]. The M_w and polydispersity index of TP-100 were 17600 and 1.3, respectively. ^{1}H NMR of TP-100 ($CDCl_3$/F113, δ): 2.39 (m, 2H), 2.73 (m, 2H), 2.81 (m, 2H), 3.64 (m, 3H).

2.3. Preparation of Polymer Thin Films. We prepared polymer thin films (≤ 100 nm thick) by spin-coating a 1 wt % solution of the TP-Xs in F113 onto a silicon wafer at 3000 rpm for 30 s using a spin-coater (Laurell model WS-400A-6NPP/LITE). The films were then dried in a vacuum oven for 24 h at room temperature. The annealing treatment was conducted through heating the polymer films at 60 °C for 2 h to compare the as-prepared and annealed films.

2.4. Analysis. The ^{1}H NMR spectra (500 MHz) were measured in either $CDCl_3$ or a $CDCl_3$/F113 mixture using a Bruker Avance 500 apparatus. The M_w and polydispersity index were obtained on a Viscotek GPC using a diffractometer as the detector. THF and F113 were used as a solvent, and monodisperse polystyrenes were used as the standards.

Differential scanning calorimetry (DSC, TA Instruments 2920 differential scanning calorimeter) was carried out at heating and cooling rates of 5 °C min^{-1}. To eliminate the effect of the thermal history on the sample transitions, all samples were heated to 200 °C and held at that temperature for 5 min before cooling. The transition temperatures and enthalpy changes were obtained from the second heating scan.

The stylus surface roughness, R_a, was obtained by atomic force microscopy (AFM). The AFM observations were performed using an SPA300HV multifunction unit/SPI3800 probe station, Seiko Instruments, Japan. The AFM images were obtained in tapping mode in air using a 20 μm × 20 μm scanner.

The molecular structure of polymer thin films could be characterized by combining the analysis of the NEXAFS and GIXD. The NEXAFS experiments were conducted at the photoemission spectroscopy 2B1 beamline (beam size = 1×3 mm^2) at the Pohang Accelerator Laboratory, Korea. The C K-edge NEXAFS spectra were recorded in partial electron yield (PEY) mode. The degree of polarization of the X-ray was 0.85, and the entrance grid bias of -210 V was used. The soft X-ray incident angles were 20 and 90° for polarization dependence. The PEY signals were normalized by the incident beam intensity obtained from the photo yield of a clean silicon surface. Details of this technique are reported elsewhere.[41−44]

GIXD patterns were obtained using a high-power X-ray beam (photon flux $\approx 10^{11}$ photons s^{-1} mrad^{-1} per 0.1%, beam size ≤ 0.5 mm^2) from a synchrotron radiation source (4C2 beamline, Pohang Accelerator Laboratory, Korea) at a wavelength $\lambda = 1.3807$ Å. The detection system was equipped with a 2-D X-ray detector (PI-SCX4300−165/2, Princeton Instrument). Details of the analytical methodology are reported elsewhere.[45,46]

The contact angles of the polymer thin film were determined using a Krüss DSA10 contact angle analyzer interfaced to a computer running drop shape analysis software. The advancing and receding contact angles were measured using drops of several liquids. The contacting liquids (water, diiodomethane (DIM), ethylene glycol (EG), benzyl alcohol (BA), octane, decane, dodecane, and hexadecane) were of the highest purity available and used as received. The contact angles for each sample were measured a minimum of five times on independently prepared films, and the average was used. The contact angle variability was within 1° for all test liquids.

3. Results and Discussion

Figure 1 shows the synthetic route of the comb-like fluorinated poly(oxyethylene)s (TP-Xs, where X is the mol % of monomeric units containing fluoroalkyl side group) prepared by a polymer analogous reaction of poly[oxy(chloromethyl)ethylene] and sodium 1*H*,1*H*,2*H*,2*H*-perfluorodecane-1-thiolate in an ionic liquid, 1-butyl-3-methyl-imidazolium chloride ([bmim][Cl]), as the reaction medium.[40] Table 1 lists the reaction conditions and degree of substitution. TP-Xs having high contents of fluoroalkyl side group could not be prepared using common organic solvents because the several highly fluorinated polymers including TP-Xs have very poor solubility in common organic solvents.[20,21,24,25,47] However, TP-Xs having high contents of fluoroalkyl side group could be prepared successfully when the ionic liquid, [bmim][Cl], was used as a reaction medium because of the ability of an ionic liquid to act as a reaction medium and catalyst, which can increase the degree of substitution in nucleophilic substitution reactions.[40,48−51] The content of fluoroalkyl side groups in TP-Xs could be controlled from 48 to 100 mol % by changing the poly[oxy(chloromethyl)ethylene] to sodium 1*H*,1*H*,2*H*,2*H*-perfluorodecane-1-thiolate mole ratios from 0.55 to 1.20. The TP-Xs having lower content of fluoroalkyl side group such as 10 and 30 mol % were also synthesized with the same procedures; however, these polymers were not soluble in F113, and we could not obtain the films for the surface analysis. The casting solvent has been known to have negligible effect on the tilt angles of fluoroalkyl groups,[18] whereas surface morphology and contact angle values have been found to be affected by casting solvent.[9,18] Therefore

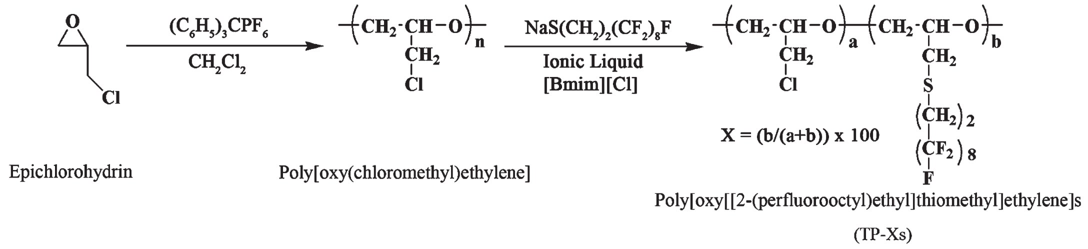

Figure 1. Synthetic Route for TP-Xs.

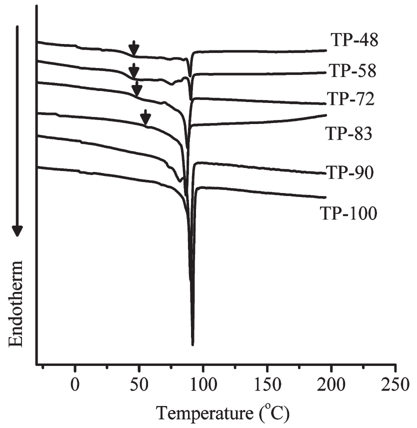

Figure 2. DSC curves of TP-Xs. (The black arrows indicate the glass-transition temperature.)

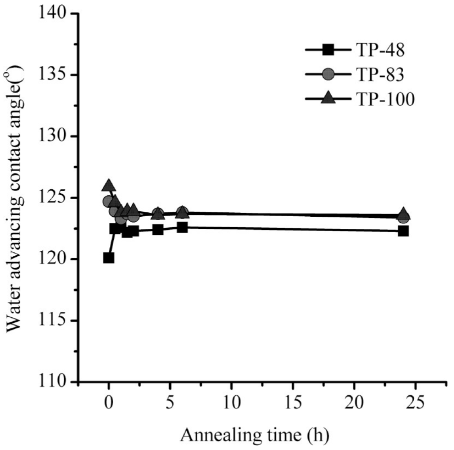

Figure 3. Water contact angles of TP-48, TP-83, and TP-100 according to annealing time. The solid lines are guides to the eye.

we decided to use only one solvent (namely, F113) to prepare the films, and thus the results from TP-Xs having fluoroalkyl side group < 48 mol % were not included.

Figure 2 shows the DSC traces of the TP-Xs obtained from the second heating scan at a heating rate of 5 °C $\min^{-1}$. Table 1 lists the transition temperatures and enthalpy changes. The glass-transition temperature (T_g) increased with increasing content of the fluoroalkyl side groups, whereas no glass transition was observed for the polymers having ≥90 mol % of fluoroalkyl side group. A long and rigid fluoroalkyl side group might reduce the mobility of the polymer backbone, thereby increasing the T_g. An attempt was made to observe the T_g of TP-90 and TP-100 by quenching the melted samples in liquid nitrogen. However, the T_g was not observed. There are some reports that the glass transition of polymers having high content of fluoroalkyl side group is not easily detected from the DSC curves.[22,25,52] For all measured polymers, endothermic peaks were observed at ~90 °C, indicating the melting transition of the fluoroalkyl side group crystallites. The transition enthalpy change values increased with increasing content of fluoroalkyl side group, possibly because of the increased inter-side-chain interactions.[13,22]

"Annealed" films were prepared from "as-prepared" films by heating to 60 °C for 2 h to observe the effect of annealing treatment on the comb-like fluorinated poly(oxyethylene) thin films having different content of fluoroalkyl side group. The annealing time was long enough to ensure thermodynamic equilibrium in the polymer thin films from a water contact angle experiment. Figure 3 shows the water advancing contact angle of the TP-Xs (48, 83, 100 mol %) according to the annealing treatment time. After a 1 h annealing treatment, all of the measured films showed constant values. The stylus surface roughness, R_a, of the thin films obtained using AFM ranged from 1.1 to 5.7 nm (Table 2). These small R_a values indicate that the surface roughness has little effect on the contact angles and can be ignored in the contact angle measurements; that is, a smooth surface (R_a < 100 nm) does not affect the contact angle of the polymer films.[53]

NEXAFS and GIXD were used to examine further the effects of the content of the fluoroalkyl side group and the annealing treatment on the TP-Xs thin films. NEXAFS is a very useful technique for determining the molecular structural ordering near the outmost surface. Moreover, the average tilt angle of side group in the comb-like polymer thin films can be estimated.[17,18,22,43,44] Figure 4 shows the NEXAFS spectra of the C 1s edge of the annealed TP-100 thin film recorded at two incidence angles using PEY mode, such as 90 (normal incidence) and 20° (grazing incidence), respectively. Peaks corresponding to the 1s-σ^* transitions for the C−H, C−F, and C−C bonds appeared at 288, 292, and 295 eV, respectively. Only the spectrum of the annealed TP-100 film is provided here as an example because all films showed similar results. The C−F bond intensity was larger at 90 than at 20°, whereas the C−C bond intensity showed an opposite behavior. This trend suggests that the fluoroalkyl side groups are oriented almost perpendicular to the film surface. The average tilt angles of the fluoroalkyl side group with the surface normal were estimated from the calculation using the peak intensities of the C−F bonds at the grazing and normal incidence angles according to the procedure used by Ober et al.[17−19,22] As shown in Table 2 and Figure 5, the average tilt angles of all TP-Xs films lay in the range from 26 to 33°, which are larger than those of the semifluorinated self-assembled monolayer but smaller than those of the comb-like fluorinated polymers reported by Ober et al.[17] and the fluorinated polystyrenes reported in our previous report.[22] This suggests that the fluoroalkyl side groups in the TP-Xs thin films have a more perpendicularly ordered structure to the film surface than the other fluorinated polymers, even though they are more tilted than the self-assembled monolayer.[17,22] The flexible oxyethylene backbone of TP-Xs could provide high mobility of fluoroalkyl side group to form well-ordered structures almost perpendicular to the film surface. The content of fluoroalkyl side group had little effect on the average tilt angles, even though the average tilt angles appeared to increase with increasing content of fluoroalkyl side group from 58 to 100 mol %, whereas the changes

Table 2. AFM, GIXD, and NEXAFS Results of TP-Xs

		AFM result	NEXAFS results			GIXD results	
		R_a (nm)	S_{C-F}[a]	$S_{F\text{-helix}}$[b]	tilt angle (°)[c]	small-angle *d* spacing (Å)[d]	wide-angle *d* spacing (Å)[e]
as-prepared films	TP-48	1.2	−0.2869	0.5738	32.21	33.6, 17.6, 11.6	4.94
	TP-58	1.3	−0.3572	0.7144	25.86	34.3, 17.8, 11.8	4.85
	TP-72	1.5	−0.3472	0.6944	26.82	34.4, 17.6, 11.8, 5.7	4.92
	TP-83	1.1	−0.3192	0.6384	29.40	32.6, 16.3, 11.0, 6.6, 5.7	4.90
	TP-90	1.6	−0.3297	0.6594	28.46	32.9, 16.9, 11.3, 6.8, 5.7	4.93
	TP-100	1.2	−0.3145	0.6290	29.82	32.1, 16.5, 11.0, 6.6, 5.5	4.90
annealed films	TP-48	3.5	−0.2835	0.5670	32.50	32.9, 16.9, 11.3 (38.4, 19.5, 13.2)[f]	4.92
	TP-58	5.7	−0.3499	0.6998	26.57	32.3, 16.7, 11.3, 5.8 (38.6, 19.5, 13.2)[f]	4.96
	TP-72	3.4	−0.3347	0.6694	28.00	34.4, 17.2, 11.5, 6.8, 5.7 (38.2, 19.3, 12.9)[f]	4.93
	TP-83	2.1	−0.3231	0.6462	29.05	32.3, 16.5, 11.2, 6.8, 5.8	4.98
	TP-90	1.6	−0.2814	0.5628	32.67	32.3, 16.5, 11.2, 6.7, 5.6	4.96
	TP-100	1.5	−0.3079	0.6158	30.41	32.1, 16.3, 11.0, 6.6, 5.6	4.96

[a] Surface orientational parameter of C−F bonds. [b] Surface orientational parameter of fluoroalkyl helix. [c] Tilt angle of fluoroalkyl helix to the surface normal. [d] Series of *d* spacings corresponding to the 001, 002, 003, 005, and 006 indices of lamellar thickness. [e] *d* Spacings representing the distance between the fluorinated alkyl side chains. [f] Additional lamellar structure.

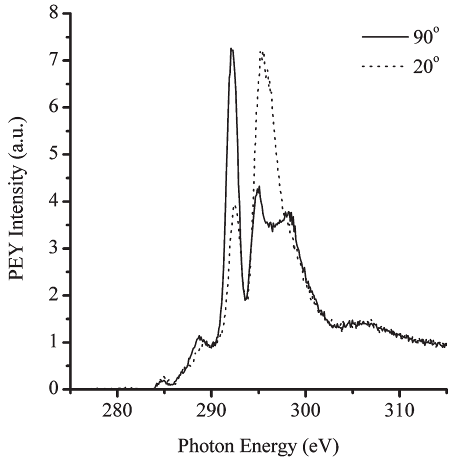

Figure 4. PEY NEXAFS spectra from the annealed TP-100 thin film at two different incidence angles.

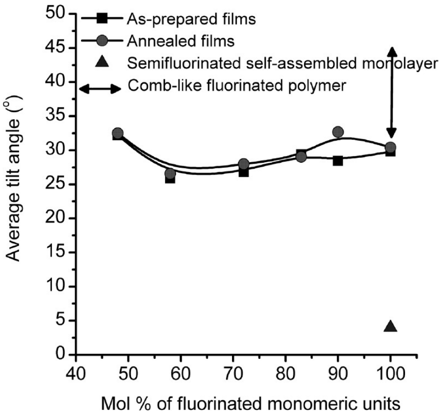

Figure 5. Average tilt angles of fluoroalkyl side group with the surface normal. Semifluorinated self-assembly monolayer and comb-like fluorinated polymer values were described in refs 17 and 22. The solid lines are guides to the eye.

are not much, if any. Furthermore, annealing treatment did not alter the average tilt angles significantly. Because the order parameter and tilt angle of the fluoroalkyl side group determined from NEXAFS represent an "average" value, it was not possible to distinguish between the case of all fluorinated groups being tilted homogeneously by the same angle and the case of disordered fluorinated groups with a wide distribution of tilt angles.[18,19,54] Moreover, the reported tilt angles, which were calculated using only two X-ray incident angles, do not take into account the effects of inelastic collisions of Auger electrons on the electron yield and compositional depth profiles[41,42] and are, therefore, only approximate values. Therefore, GIXD was carried out to distinguish and quantify the difference in molecular structural ordering and orientation of the TP-Xs thin films.

The 2-D GIXD patterns of the TP-Xs were recorded using a synchrotron X-ray beam at an incident angle of 0.17° (Figure 6). Table 2 lists the out-of-plane (small-angle) and in-plane (wide-angle) *d* spacings obtained from the 2-D GIXD patterns. The out-of-plane diffraction patterns in the small-angle region showed a series of peaks corresponding to the (00*h*) indices, indicating that all thin films have lamellar structures oriented parallel to the film surface. The *d* spacing of the (00*h*) reflection were similar to those of all films with lamellar thickness of 32−34 Å and was approximately double that of the expected fluoroalkyl side group length, assuming that the side groups are fully extended in the trans conformation.[13,22] The number of peaks from the out-of-plane scattering increased with increasing content of fluoroalkyl side group. For example, peaks for the (005) and (006) planes were observed from the as-prepared films containing > 72 mol % of fluoroalkyl side group and annealed films containing > 58 mol % of fluoroalkyl side group. Therefore, we obtained polymer films having more ordered lamellar structures by increasing the content of the fluoroalkyl side group and by annealing treatment, even though these thin films have similar *d* spacings. In the case of TP-Xs having ≤72 mol % of fluoroalkyl side group, an additional lamellar structure with a slightly larger *d* spacing than that of the original lamellar structure was observed after the annealing treatment. This additional lamellar structure appears to be generated by phase separation between the hydrocarbon-rich and fluorocarbon-rich domains. Similar additional large lamellar structures were previously observed in comb-like polyacrylates having small contents of fluoroalkyl side group.[23]

The in-plane diffraction patterns shown in the wide-angle regions originated from the ordering of fluoroalkyl side group also showed a similar tendency. The intermolecular distances of the fluoroalkyl side group were similar (4.9 Å), which is the same as the intermolecular distance of the polytetrafluoroethylene crystals with the closest hexagonal packing of fluoroalkyl group.[55,56] This suggests that fluoroalkyl side groups on the polymer surface of both the as-prepared and annealed films have the closest hexagonal packing structures, regardless of the content of fluoroalkyl side group and annealing treatment. The flexible oxyethylene backbone in TP-Xs may provide high mobility of fluoroalkyl side group to form ordered packing structures, which in turn show hexagonally ordered fluoroalkyl side group structures despite their differences in the content of fluoroalkyl side group. The

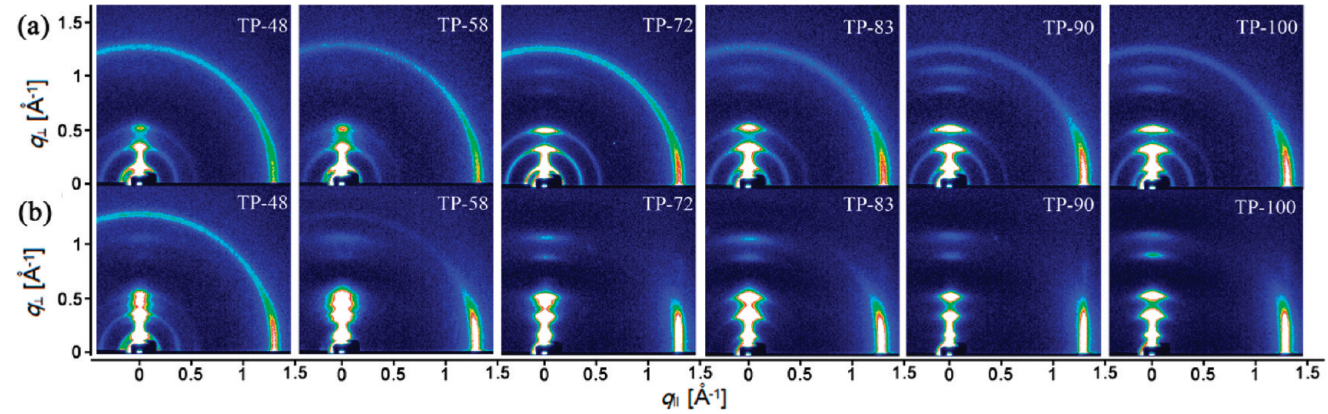

Figure 6. Two-dimensional GIXD patterns of the (a) as-prepared films and (b) annealed films.

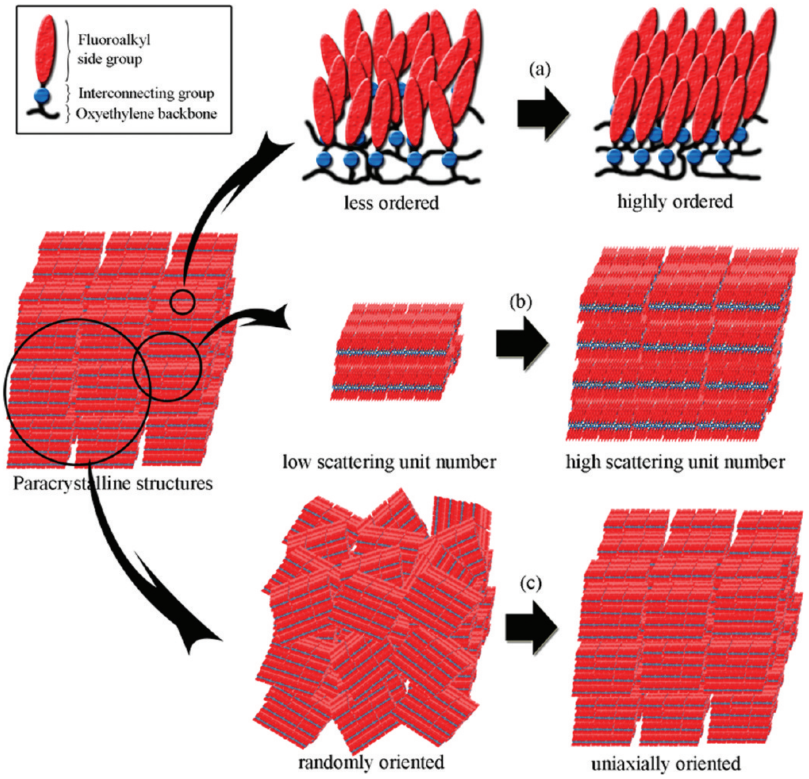

Figure 7. Schematic diagram for the changes of paracrystalline structure (a) ordering, (b) scattering unit number, and (c) orientation.

peaks from the out-of plane and in-plane scattering became sharper, and their intensities increased, with increasing content of fluoroalkyl side group. These GIXD patterns reveal that the fluoroalkyl side groups and lamellar structures were oriented perpendicular and parallel to the film surface, respectively, and more ordered molecular structures were obtained with increasing the content of fluoroalkyl side group, even though the out-of-plane and in-plane *d* spacings were identical.

Paracrystalline structure analysis was carried out using the Hosemann paracrystal model[29,30] to quantify further the difference in molecular structure of the TP-Xs. The Hosemann paracrystal model is considered to be the most suitable model to determine the polymer structures having lamellar structures.[13,14,31,32] The paracrystalline structure ordering, scattering unit number, and orientation could be derived from the 2-D GIXD patterns. Figure 7 shows a schematic diagram of the changes in the paracrystalline structure on the TP-Xs thin films. Paracrystalline structure ordering and scattering unit number were calculated using the reflection peaks in the small-angle region, and a paracrystalline structure orientation was observed on the 2-D GIXD patterns.

For a paracrystalline system, the paracrystalline lattice factor $Z(s)$ of the hth-order reflection can be determined by the following

$$Z(s) = Z(h) = [1 - \exp(-4\pi^2 g^2 h^2)]/ \\ [(1 - \exp(-2\pi^2 g^2 h^2))^2 + (4\sin^2 2\pi h)\exp(-2\pi^2 g^2 h^2)] \quad (1)$$

where s is the reciprocal lattice vector and g is the standard deviation of the Gaussian distribution divided by the average lattice vector $\tilde{a}$. g is a parameter used to evaluate the degree of paracrystalline structure disorder. The value of g is given experimentally by the following

$$(\delta\beta)^2 = (1/\tilde{a}^2)[(1/N^2) + \pi^4 g^4 h^4] \quad (2)$$

where $\delta\beta$ is the integral breadth of a reflection, h is the scattering order, and N is the number of scattering units.[13,14] A linear relationship between $(\delta\beta)^2$ and h^4 could be obtained from the

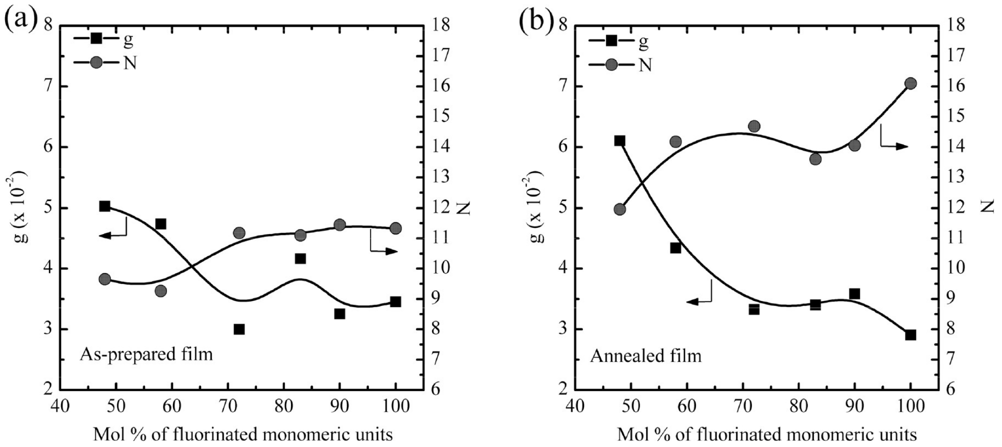

Figure 8. Paracrystalline structure disorder parameter (g) and number of scattering unit (N) values for (a) as-prepared films and (b) annealed films. The solid lines are guides to the eye.

out-of-plane (001), (002), and (003) reflections of TP-Xs, and the g and N values were calculated using eq 2.

As shown in Figure 8, the paracrystalline structure disorder parameter g decreased with increasing content of fluoroalkyl side group, indicating that the level of paracrystalline structure ordering increases with increasing content of fluoroalkyl side group. In addition, the as-prepared films containing > 72 mol % of fluoroalkyl side group and annealed films containing > 58 mol % of fluoroalkyl side group have very low g values. However, the g values of the as-prepared films and annealed films with a same content of fluoroalkyl side groups were similar except for TP-48. The higher g value in TP-48 after annealing treatment might be caused by the additional lamellar structure produced after annealing treatment, as described above. Previously, the g values of poly(fluoroalkyl acrylate)[13] and poly(fluoroalkyl methacrylate)[14] films were found to decrease after annealing treatment, which is different from the TP-Xs in this study. Because the TP-Xs have a flexible oxyethylene backbone, highly ordered paracrystalline structures (smaller g values) could be easily prepared from the spin coating process. Therefore, the annealing treatment does not change the g values considerably. Such highly ordered paracrystalline structures on the surface could not be obtained for the poly(fluoroalkyl acrylate)s and poly(fluoroalkyl methacrylate)s from the spin coating process because the backbone is not flexible enough, whereas the highly ordered surface structures were obtained after annealing treatment. Therefore, the g values of both the as-prepared and the annealed TP-100 are similar to those of annealed poly(fluoroalkyl acrylate) and poly(fluoroalkyl methacrylate).[13,14] The g values of the TP-Xs indicate that the paracrystalline structure ordering of the as-prepared films containing > 72 mol % of fluoroalkyl side group and annealed films containing > 58 mol % of fluoroalkyl side group are sufficiently high.

In the case of the N values, meaning the number of scattering unit, the as-prepared films containing > 72 mol % of fluoroalkyl side group and the annealed films containing > 58 mol % of fluoroalkyl side group have larger scattering unit numbers than the other TP-Xs having lower content of fluoroalkyl side group. Therefore, the ordering and scattering unit number of the paracrystalline structure increase with increasing contents of fluoroalkyl side group. The scattering unit numbers show plateau values when the contents of side group are > 72 mol % in as-prepared films, and annealed films having > 58 mol % content of fluoroalkyl side group show higher N values compared with the other films. After annealing treatment, paracrystalline structure ordering represented by the g value does not change significantly, whereas the scattering unit number increases, indicating that highly ordered paracrystalline structures have large “building blocks”.

The 2-D GIXD patterns can provide information on the orientation of paracrystalline structure. If the paracrystalline structures are randomly oriented within the film, the 2-D GIXD pattern consists of isotropic Debye–Scherrer diffraction rings rather than diffraction spots because of linkages of the diffraction spots from the same family of lattice planes.[31,32,44] Because the paracrystalline structures are uniaxially oriented in a certain direction, the scattering ring patterns become weaker and form spots with a single orientation. As shown in Figure 6, all of the as-prepared and annealed TP-48 films showed clear ring patterns in both the small- and wide-angle regions, indicating that the orientation of the paracrystalline structure is poor. As the content of fluoroalkyl side group was increased, their ring patterns became weaker and uniaxially oriented, but the ring patterns still remained, even for as-prepared TP-100. However, after the annealing treatment, polymer thin films having ≥58 mol % of fluoroalkyl side group showed sharp and condensed peak patterns, indicating that the paracrystalline structures in the films are uniaxially oriented. Therefore, the annealed TP-Xs thin films containing ≥58 mol % of fluoroalkyl side group have highly ordered and uniaxially oriented paracrystalline structures with high scattering unit number.

The polymer surface properties, such as the surface energy and surface stability, have been known to be related to the surface molecular structures.[7−16,22,24,38] In particular, highly ordered and uniaxially oriented paracrystalline structures with high scattering unit number (annealed TP-Xs containing ≥58 mol % of fluoroalkyl side group) were expected to show low surface energy and good surface stability. Taking the molecular structural analysis results into account, the surface energy and stability were further characterized in detail by the contact angle measurement. Table 3 shows the advancing contact angles and hysteresis of the TP-Xs thin films using various test liquids. The advancing and receding contact angles were measured using eight kinds of liquid from water, with the highest surface tension, to octane, with the lowest surface tension. The contact angle hysteresis (H) is the difference between the advancing and receding contact angle values. The correlation between the contact angle and surface energy is still controversial, and none of the methods proposed are generally accepted.[57,58] Normally, two or three test liquids are used for the contact angle measurements, which are then used to obtain the surface energy. In these cases, the surface energies vary according to the types of liquid used for the measurements.[22,58] Table S1 in Supporting Information lists the surface energies of the TP-Xs obtained by applying the advancing contact angle results to

Table 3. Advancing Contact Angles and Hysteresis of TP-Xs Using Various Test Liquids

		contact angle, θ, (hysteresis) [deg]							
		water	DIM[a]	EG[b]	BA[c]	octane	decane	dodecane	hexadecane
as-prepared films	TP-48	120.1(20.7)	96.7(26.5)	[d]	[d]	70.9(13.5)	75.4(10.7)	78.1(11.5)	81.0(9.8)
	TP-58	123.1(24)	96.9(27.2)	[d]	[d]	71.0(18.6)	75.4(11.6)	78.2(15.4)	81.7(13)
	TP-72	124.3(24.2)	96.9(25.6)	[d]	91.7(22.2)	71.7(14.5)	75.9(12.6)	78.9(16.5)	81.8(14.1)
	TP-83	124.7(25.3)	96.7(26.4)	[d]	93.4(30.6)	71.7(16.6)	76.5(14.1)	78.8(17.1)	83.0(16.8)
	TP-90	125.3(24.5)	97.9(28.3)	[d]	92.8(26.2)	71.8(12.7)	76.3(14.2)	78.8(17.8)	82.1(14.9)
	TP-100	125.9(26.3)	97.3(27.1)	[d]	91.5(22.3)	71.3(11)	75.2(14.1)	78.3(17.5)	81.9(16.5)
annealed films	TP-48	122.3(21.6)	97.9(23)	[d]	[d]	71.1(10.5)	75.4(8)	78.8(10.6)	81.3(13.2)
	TP-58	122.0(26)	100.6(33.1)	105.4(27.4)	94.6(42.3)	72.7(12.4)	77.3(10.2)	81.6(11.8)	85.6(10.1)
	TP-72	123.4(22)	100.4(14.5)	105.2(27)	95.5(33.9)	73.2(12)	77.4(7.5)	81.2(8.7)	85.2(8.8)
	TP-83	123.5(23.1)	100.4(27.2)	105.1(32)	93.3(31)	72.4(11.2)	76.9(11.3)	80.0(13.4)	83.8(16.2)
	TP-90	123.0(24.6)	100.4(16.1)	104.4(26.4)	93.9(30.4)	72.4(9.4)	77.0(7)	80.4(7.8)	85.1(10.8)
	TP-100	123.7(24.1)	100.2(15.4)	104.6(27.2)	94.0(26.5)	72.9(9.5)	77.1(6.6)	80.9(7.7)	84.9(9.6)

[a] Diiodomethane. [b] Ethylene glycol. [c] Benzyl alcohol. [d] Measurement was not possible because polymer film is partially soluble in EG and BA.

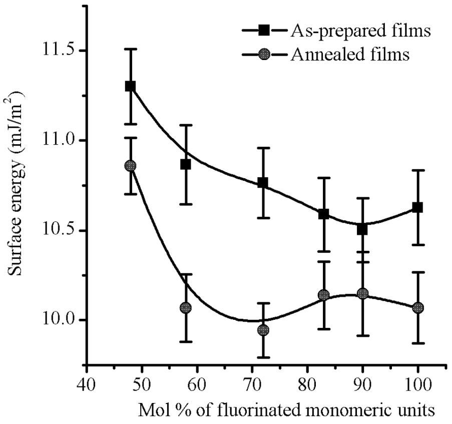

Figure 9. Surface energy obtained from equation of state approach of the TP-Xs. The solid lines are guides to the eye.

surface tension component theory (acid−base (van Oss) approach and equation of state approach) using various test liquid systems. The acid−base approach involves three different surface tension components, that is, the Lifshitz−van der Waals dispersive component, γ^{LW}, polar Lewis acid component, γ^{+}, and polar Lewis base component, γ^{-}, such that the total surface energy, γ^{total}, can be given by the following equation

$$\gamma_{\mathrm{i}}^{\mathrm{total}} = \gamma_{\mathrm{i}}^{\mathrm{LW}} + 2(\gamma_{\mathrm{i}}^{+}\gamma_{\mathrm{i}}^{-})^{1/2} \tag{3}$$

which leads to a Young's equation of the following form

$$\gamma_{\mathrm{l}}(1+\cos\theta) = 2(\gamma_{\mathrm{l}}^{\mathrm{LW}}\gamma_{\mathrm{s}}^{\mathrm{LW}})^{1/2} + 2(\gamma_{\mathrm{l}}^{+}\gamma_{\mathrm{s}}^{-})^{1/2} + 2(\gamma_{\mathrm{l}}^{-}\gamma_{\mathrm{s}}^{+})^{1/2} \tag{4}$$

This approach requires contact angle values from at least three test liquids. The trend of surface energies shows that annealed TP-Xs films containing ≥58 mol % of fluoroalkyl side group have lower surface energies than the other films, even though these values varied from 8.54 to 10.97 mJ/m^2 when different liquid systems were used (Table S1, Supporting Information). These different values were generated by a liquid−surface interaction, surface reconstruction, or both depending on the polarity of the test liquid.[22,57−59] To estimate the intrinsic surface energy of a solid, we adopted an equation of state approach that Kwok and Neumann derived an expression using eq 5. With the other commonly used methods, only one intrinsic surface energy can be obtained by the equation of state approach using eq 5 because this approach is based on the equation of state relating the surface energy of a liquid (γ_{lv}) and solid (γ_{sv}).[58,59]

$$\cos\theta = -1 + 2(\gamma_{\mathrm{sv}}/\gamma_{\mathrm{lv}})^{1/2}(1-\beta_1(\gamma_{\mathrm{lv}}-\gamma_{\mathrm{sv}})^2) \tag{5}$$

We evaluated the intrinsic surface energy of solid by curve fitting method using the eight kinds of test liquids. Figure S1 in Supporting Information shows the best fit in eq 5 for as-prepared and annealed TP-Xs films. The correlation between surface tension of test liquids and contact angles on each surface determined the intrinsic surface energy of polymer films. The γ_{sv} value of the polymer film was determined using γ_{lv}, and the contact angle (θ) was determined from the line of best fit in eq 5. β_1 is a constant value, 0.0001057.[58] Figure 9 shows the calculated surface energies. The surface energies of the annealed films are smaller than those of the as-prepared films when they have the same fluoroalkyl side group content. In addition, the surface energy generally decreases with increasing content of fluoroalkyl side group. In particular, the annealed TP-Xs containing ≥58 mol % of fluoroalkyl side groups have lower surface energies than the other TP-Xs in the range of 9.9 to 10.2 mJ m^{-2}. This behavior follows to some degree the changes in the number of scattering units, N value, and paracrystalline structure orientation measured from the 2-D GIXD patterns. After annealing treatment, the N values of the TP-Xs containing ≥58 mol % of fluoroalkyl side group increased, and the GIXD patterns became sharper without ring patterns. The as-prepared films containing ≥72 mol % of fluoroalkyl side group having less sharper GIXD patterns with some ring patterns have larger surface energies than the annealed films containing ≥58 mol % of fluoroalkyl side group (Figure 6), even though they have similar paracrystalline structure ordering, as represented by the g values. The surface energy behavior does not follow the changes in the average tilt angle, lamellar thickness, and the interchain distance of fluoroalkyl side group. These values did not change significantly after annealing treatment and are less affected by the content of fluoroalkyl side group. As previously mentioned, the g values of all TP-Xs containing ≥58 mol % of fluoroalkyl side groups are close to those of other annealed comb-like fluorinated polymers with highly ordered structures. The interchain distance of the fluoroalkyl side group of TP-Xs is the same as the intermolecular distance of the polytetrafluoroethylene crystals with the closest hexagonal packing of fluoroalkyl group, and the tilt angles of the TP-Xs are even smaller than those of the other comb-like fluorinated polymers.[13,14,17,55,56] Therefore, these TP-Xs values are already the minimum values for fluorinated polymers. Therefore, further annealing treatment cannot lower them further. However, the N values and paracrystalline structure orientation measured from 2-D GIXD patterns change after annealing treatment. Therefore, a further decrease in surface energy with increasing content of fluoroalkyl side group of the TP-Xs and after annealing treatment could be correlated with the N values and paracrystalline structure orientation measured from the 2-D GIXD patterns. The surface energies of TP-Xs are affected by paracrystalline structure ordering, orientation, and scattering unit number. In the case of annealed TP-48 and as-prepared TP-100 films, the as-prepared TP-100 film shows smaller surface energy value than the annealed TP-48 film despite of its lower scattering unit number. This phenomenon could be explained by the *g* value (paracrystalline ordering) trend. The *g* value of the annealed TP-48 is larger than that of the as-prepared TP-100. Large *g* value means a poor paracrystalline structure ordering. TP-Xs having > 58 mol % of fluoroalkyl side groups show very small g values. However, TP-48 shows a larger *g* value than other TP-Xs, so it has larger surface energy value. This result indicates that both small *g* and large *N* values are required for the surfaces to have the small surface energy. If the *g* values are sufficiently small, then the *N* value and paracrystalline orientation become important parts to determine the surface energy as the annealed TP-Xs films having ≥58 mol % of fluoroalkyl side group.

The annealed TP-Xs films having ≥58 mol % of fluoroalkyl side group also showed high surface stability against the polar test liquids during the contact angle experiment. As shown in Table 3, some of the contact angles are not available from EG or BA. The contact angles of EG could not be obtained on all of the as-prepared films and annealed TP-48 because these liquids smeared into these polymer films, possibly because of the partial miscibility of EG with these polymers films. However, the contact angles of EG on the annealed TP-Xs thin films, which have highly ordered and uniaxially oriented paracrystalline structures with high scattering unit number, could be measured because of the improved surface structural stability. In the case of BA, although the stability difference is not as significant as that in the case of EG, BA was found to smear in polymer films containing lower contents of fluoroalkyl side groups, such as as-prepared TP-48 and TP-58 and annealed TP-48. This stability also follows the changes in surface energy, *N* values, and paracrystalline structure orientation measured from the 2-D GIXD patterns.

4. Conclusions

Comb-like fluorinated poly(oxyethylene)s having different content of fluoroalkyl side group were characterized by NEXAFS, GIXD, and contact angle measurements to correlate the surface properties with their molecular structures. There was no strong correlation between the contents of fluoroalkyl side groups and the tilt angle of the side chains. The *d* spacing of all comb-like fluorinated poly(oxyethylene)s was very similar, even though the polymers have different contents of fluoroalkyl side groups. Furthermore, these values did not change after annealing treatment. The paracrystalline structure ordering represented by the *g* value also did not change after annealing treatment, whereas the *g* values of the as-prepared films having ≥72 mol % of fluoroalkyl side group and the annealed films having ≥58 mol % of fluoroalkyl side group were smaller (better paracrystalline structure ordering) than those with a smaller amount of fluoroalkyl side groups. The *d*-spacing values, *g* values, and tilt angles of the comb-like fluorinated poly(oxyethylene)s were close to or even lower than the other fluorinated polymers. Therefore, further changes in the tilt angles, *d*-spacing values, and *g* values were not possible, so they do not represent the changes in the surface energy of the comb-like fluorinated poly(oxyethylene)s according the content of the fluoroalkyl side group and after annealing treatment. However, the surface properties follow the changes in the number of scattering units, which are represented by the *N* value and paracrystalline structure orientation measured from the 2-D GIXD patterns. For example, annealed polymer thin films having ≥58 mol % of fluoroalkyl side group showed uniaxially oriented paracrystalline structures with a large *N* value. In addition, these films showed high surface stability with a very low surface energy in the range of 9.9 to 10.2 mJ/m^2 calculated using the equation of state approach. The surface energy of the annealed polymer film having < 58 mol % of fluoroalkyl side group and those of all as-prepared films having less oriented paracrystalline structures and smaller *N* value are > 10.5 mJ/m^2. Therefore, the orientation of the paracrystalline structure and *N* value are important parameters to have a strong correlation with the surface energy of comb-like fluorinated poly(oxyethylene)s. This is believed to be the first report to show a clear relationship between the surface properties and the orientation of the paracrystalline structure and scattering unit number.

Acknowledgment. This work was financially supported by Korea Atomic Energy for Research Institute (KAERI, 2009-0078292), the project titled "Development of new restoration technology for marine environment" of the Ministry of Land, Transport and Maritime Affairs, Korea, and Korea Science and Engineering Foundation (KOSEF) grant by Korean government (MEST) (grant code: R2009-007711). Experiments at Pohang Accelerator Laboratory were partially supported by MOST and POSTECH.

Supporting Information Available: Surface energy (acid−base and equation of state approach) of the TP-Xs and γ_{lv} versus $\gamma_{lv}\cos\theta$ for the equation of state approach on the (a) as-prepared and (b) annealed TP-Xs. This material is available free of charge via the Internet at http://pubs.acs.org.

References and Notes

(1) Hougham, G. In *Fluoropolymers*; Hougham, G., et al., Eds.; Plenum Press: New York, 1999.

(2) *Modern Fluoropolymers: High Performance Polymers for Diverse Applications*; Scheirs, J., Ed.; Wiley: New York, 1997.

(3) Lee, S.; Park, J.-S.; Lee, T. R. *Langmuir* **2008**, *24*, 4817–4826.

(4) Schmidt, D. L.; Coburn, C. E.; Dekoven, B. M.; Potter, G. E.; Meyers, G. F.; Fisher, D. A. *Nature* **1994**, *368*, 39–41.

(5) Bryan-Brown, G. P.; Wood, E. L.; Sage, I. C. *Nature* **1999**, *399*, 338–340.

(6) Ober, C. K.; Gabor, A. H.; Gallagher-Wetmore, P.; Allen, R. D. *Adv. Mater*. **1997**, *9*, 1039–1043.

(7) Tsibouklis, J.; Nevell, T. G. *Adv. Mater*. **2003**, *15*, 647–650.

(8) Tsibouklis, J.; Graham, P.; Eaton, P. J.; Smith, J. R.; Nevell, T. G.; Smart, J. D.; Ewen, R. J. *Macromolecules* **2000**, *33*, 8460–8465.

(9) Urushihara, Y.; Nishino, T. *Langmuir* **2005**, *21*, 2614–2618.

(10) Park, I. J.; Lee, S. B.; Choi, C. K. *Macromolecules* **1998**, *31*, 7555–7558.

(11) Hirao, A.; Sugiyama, K.; Yokoyama, H. *Prog. Polym. Sci.* **2007**, *32*, 1393–1438.

(12) Matsunaga, M.; Suzuki, T.; Yamamoto, K.; Hasegawa, T. *Macromolecules* **2008**, *41*, 5780–5784.

(13) Honda, K.; Morita, M.; Otsuka, H.; Takahara, A. *Macromolecules* **2005**, *38*, 5699–5705.

(14) Honda, K.; Morita, M.; Sakata, O.; Sasaki, S.; Takahara, A. *Macromolecules* **2010**, *43*, 454–460.

(15) Yamaguchi, H.; Honda, K.; Kobayashi, M.; Morita, M.; Masunaga, H.; Sakata, O.; Sasaki, S.; Takahara, A. *Polym. J.* **2008**, *40*, 854–860.

(16) Wang, J.; Mao, G.; Ober, C. K.; Kramer, E. J. *Macromolecules* **1997**, *30*, 1906–1914.

(17) Genzer, J.; Sivaniah, E.; Kramer, E. J.; Wang, J.; Körner, H.; Xiang, M.; Char, K.; Ober, C. K.; DeKoven, B. M.; Bubeck, R. A.; Chaudhury, M. K.; Sambasivan, S.; Fischer, D. A. *Macromolecules* **2000**, *33*, 1882–1887.

(18) Genzer, J.; Sivaniah, E.; Kramer, E. J.; Wang, J.; Xiang, M.; Char, K.; Ober, C. K.; Bubeck, R. A.; Fischer, D. A.; Graupe, M.; Colorado, R., Jr.; Shmakova, O. E.; Lee, T. R. *Macromolecules* **2000**, *33*, 6068–6077.

(19) Li, X.; Andruzzi, L.; Chiellini, E.; Galli, G.; Ober, C. K.; Hexemer, A.; Kramer, E. J.; Fischer, D. A. *Macromolecules* **2002**, *35*, 8078–8087.

(20) Krishnan, S.; Ayothi, R.; Hexemer, A.; Finlay, J. A.; Sohn, K. E.; Perry, R.; Ober, C. K.; Kramer, E. J.; Callow, M. E.; Callow, J. A.; Fischer, D. A. *Langmuir* **2006**, *22*, 5075–5086.

(21) Busch, P.; Krishnan, S.; Paik, M.; Toombes, G. E. S.; Smilgies, D.-M.; Gruner, S. M.; Ober, C. K. *Macromolecules* **2007**, *40*, 81–89.

(22) Kim, B. G.; Chung, J.-S.; Sohn, E.-H.; Kwak, S.-Y.; Lee, J.-C. *Macromolecules* **2009**, *42*, 3333–3339.

(23) de Crevoisier, G.; Fabre, P.; Leibler, L.; Tence-Girault, S.; Corpart, J. M. *Macromolecules* **2002**, *35*, 3880–3888.

(24) Kim, B. G.; Sohn, E.-H.; Cho, K.; Lee, J.-C. *Eur. Polym. J.* **2008**, *44*, 2912–2919.

(25) Paik, M. Y.; Krishnan, S.; You, F.; Li, X.; Hexemer, A.; Ando, Y.; Kang, S. H.; Fischer, D. A.; Kramer, E. J.; Ober, C. K. *Langmuir* **2007**, *23*, 5110–5119.

(26) Liu, Y.; Nagle, J. F. *Phys. Rev. E.* **2004**, *69*, 040901.

(27) Pabst, G.; Rappaolt, M.; Amenitsch, H.; Laggner, P. *Phys. Rev. E.* **2000**, *62*, 4000–4009.

(28) Yakabe, H.; Sasaki, S.; Sakata, O.; Takahara, A.; Kajiyama, T. *Macromolecules* **2003**, *36*, 5905–5907.

(29) Lindenmeyer, P. H.; Hosemann, R. *J. Appl. Phys.* **1963**, *34*, 42–45.

(30) Hosemann, R.; Hindeleh, A. M. *J. Macromol. Sci., Part B: Phys.* **1995**, *B34*, 327–356.

(31) Yoon, J.; Jin, K. S.; Kim, H. C.; Kim, G.; Heo, K.; Jin, S.; Kim, J.; Kim, K.-W.; Ree, M. *J. Appl. Crystallogr.* **2007**, *40*, 476–488.

(32) Yoon, J.; Lee, S. W.; Choi, S.; Heo, K.; Jin, K. S.; Jin, S.; Kim, G.; Kim, J.; Kim, K.-W.; Kim, H.; Ree, M. *J. Phys. Chem. B.* **2008**, *112*, 5338–5349.

(33) Lee, J.-C.; Litt, M. H.; Rogers, C. E. *Macromolecules* **1997**, *30*, 3766–3774.

(34) Lee, J.-C.; Litt, M. H.; Rogers, C. E. *Macromolecules* **1998**, *31*, 2440–2446.

(35) Lee, J.-C.; Oh, K.; Lee, H. B.; Kim, Y. G.; Jho, J. Y.; Kwak, S.-Y.; Park, S.-Y.; Farmer, B. L. *Macromol. Rapid Commun.* **2001**, *22*, 815–819.

(36) Lee, J.-C.; Lim, M.-Y.; Oh, K.; Lee, H. B.; Kim, Y. G.; Park, S.-Y.; Farmer, B. L. *Polymer* **2002**, *43*, 7051–7061.

(37) Lee, J.-C.; Han, S.-H.; Cha, S. H.; Park, S.-Y.; Farmer, B. L. *Polymer* **2003**, *44*, 7413–7425.

(38) Kim, B. G.; Sohn, E.-H.; Lee, J.-C. *Macromol. Chem. Phys.* **2007**, *208*, 1011–1019.

(39) Kim, B. G.; Moon, J.-K.; Sohn, E.-H.; Lee, J.-C. *Macromol. Res.* **2008**, *16*, 36–44.

(40) Kim, B. G.; Sohn, E.-H.; Chung, J.-S.; Kwak, S.-Y.; Lee, J.-C. *J. Appl. Polym. Sci.* **2009**, *114*, 132–138.

(41) Sohn, K. E.; Dimitriou, M. D.; Genzer, J.; Fischer, D. A.; Hawker, C. J.; Kramer, E. J. *Langmuir* **2009**, *25*, 6341–6348.

(42) Krishnan, S.; Paik, M. Y.; Ober, C. K.; Martinelli, E.; Galli, G.; Sohn, K. E.; Kramer, E. J.; Fischer, D. A. *Macromolecules* **2010**, *43*, 4733–4743.

(43) Stohr, J. *NEXAFS Spectroscopy*; Springer Series in Surface Sciences *25*; Springer-Verlag: Berlin, 1992.

(44) Zubavichus, Y.; Shaporenko, A.; Grunze, M.; Zharnikov, M. *J. Phys. Chem. B* **2006**, *110*, 3420–3427.

(45) Lee, B.; Park, Y.-H.; Hwang, Y.-T.; Oh, W.; Yoon, J.; Ree, M. *Nat. Mater.* **2005**, *4*, 147–151.

(46) Yoon, J.; Kim, K.-W.; Kim, J.; Heo, K.; Jin, K. S.; Jin, S.; Shin, T. J.; Lee, B.; Rho, Y.; Ahn, B.; Ree., M. *Macromol. Res.* **2008**, *16*, 575–585.

(47) Anton, D. *Adv. Mater.* **1998**, *10*, 1197–1205.

(48) Ranu, B. C.; Jana, R. *Adv. Synth. Catal.* **2005**, *347*, 1811–1818.

(49) Kim, D. W.; Song, C. E.; Chi, D. Y. *J. Am. Chem. Soc.* **2002**, *124*, 10278–10279.

(50) Lourenco, N. M. T.; Afonso, C. A. M. *Tetrahedron* **2003**, *59*, 789–794.

(51) Lee, S.; Zhang, Y. J.; Piao, J. Y.; Yoon, H.; Song, C. E.; Choi, J. H.; Hong, J. *Chem. Commun.* **2003**, 2624–2625.

(52) Shimizu, T.; Tanaka, Y.; Kutsumizu, S.; Yano, S. *Macromolecules* **1996**, *29*, 156–164.

(53) Busscher, H. J.; van Pelt, A. W. J.; de Boer, P.; de Jong, H. P.; Arends, J. J. *Colloids Surf.* **1984**, *9*, 319–331.

(54) Genzer, J.; Efimenko, K.; Fischer, D. A. *Langmuir* **2006**, *22*, 8532–8541.

(55) Volkov, V.; Plate, N.; Takahara, A.; Kajiyama, T.; Amaya, N.; Murata, Y. *Polymer* **1992**, *33*, 1316–1320.

(56) Corpart, J. M.; Girault, S.; Juhue, D. *Langmuir* **2001**, *17*, 7237–7244.

(57) Martinelli, E.; Menghetti, S.; Galli, G.; Glisenti, A.; Krishnan, S.; Paik, M. Y.; Ober, C. K.; Smilgies, D.-M.; Fischer, D. A. *J. Polym. Sci., Part A: Polym. Chem.* **2009**, *47*, 267–284.

(58) Kwok, D. Y.; Neumann, A. W. *Adv. Colloid Interface Sci.* **1999**, *81*, 167–249.

(59) Tavana, H.; Neumann, A. W. *Adv. Colloid Interface Sci.* **2007**, *132*, 1–32.